

Ions in Mixed Dielectric Solvents: Density Profiles and Osmotic Pressure between Charged Interfaces

Dan Ben-Yaakov and David Andelman*

Raymond and Beverly Sackler School of Physics and Astronomy, Tel Aviv University,
Ramat Aviv, Tel Aviv 69978, Israel

Daniel Harries

Institute of Chemistry and The Fritz Haber Research Center, The Hebrew University, Jerusalem 91904, Israel

Rudi Podgornik

Department of Theoretical Physics, J. Stefan Institute, and Department of Physics, Faculty of Mathematics and Physics, University of Ljubljana, 1000 Ljubljana, Slovenia, and Laboratory of Physical and Structural Biology, Eunice Kennedy Shriver National Institute of Child Health and Human Development, National Institutes of Health, Bethesda, Maryland 20814-0924

Received: January 13, 2009; Revised Manuscript Received: February 7, 2009

The forces between charged macromolecules, usually given in terms of osmotic pressure, are highly affected by the intervening ionic solution. While in most theoretical studies the solution is treated as a homogeneous structureless dielectric medium, recent experimental studies concluded that, for a bathing solution composed of two solvents (binary mixture), the osmotic pressure between charged macromolecules is affected by the binary solvent composition. By adding local solvent composition terms to the free energy, we obtain a general expression for the osmotic pressure, in planar geometry and within the mean-field framework. The added effect is due to the permeability inhomogeneity and nonelectrostatic short-range interactions between the ions and solvents (preferential solvation). This effect is mostly pronounced at small distances and leads to a reduction in the osmotic pressure for macromolecular separations of the order 1–2 nm. Furthermore, it leads to a depletion of one of the two solvents from the charged macromolecules (modeled as planar interfaces). Lastly, by comparing the theoretical results with experimental ones, an explanation based on preferential solvation is offered for recent experiments on the osmotic pressure of DNA solutions.

I. Introduction

The interactions between charged macromolecules immersed in aqueous solutions are of great importance in biology and material science. Because of their relevance to colloidal suspensions and biological macromolecules, the forces between charged objects mediated by electrolytes have been the focus of numerous studies.^{1–9} Within the context of the so-called primitive model, the solvent is modeled as a homogeneous dielectric medium^{9–12} affecting the system only through the dielectric constant that acts to reduce the strength of the electrostatic field. More recently, theoretical and experimental approaches, studying interactions between charged macromolecules, have been extended to also treat binary solvent mixtures.^{13–16}

The thermodynamics of binary solutions is well understood and has been described in detail in many textbooks.¹⁷ However, there are still open questions concerning the behavior of binary solutions in the presence of other degrees of freedom, such as dissolved ions and external electric fields. These additional couplings are relevant to a broader spectrum of applications, extending from manipulation of microfluids^{18–21} to biologically motivated problems such as protein stability and conformational changes.^{22–26} For example, in recent experiments, the transition

of a DNA molecule from elongated coil to compact globule was found to depend on the addition of another polarizable solvent to the aqueous solution,²⁷ suggesting that the interaction between DNA segments is modified by the presence of this additional solvent.

The effects of adding cosolvents to aqueous solutions of charged macromolecules can be quite pronounced. In fact, one of the common ways to precipitate DNA involves adding an excess amount of ethanol to the aqueous solution, which counteracts the repulsion between charged DNA strands.^{4–6} This effect has been commonly attributed to the change in solution dielectric constant. However, studies over the past decade convincingly demonstrated that alcohol changes the disjoining (i.e., the interaction) pressure between DNA strands to a much greater extent than would be expected from the direct change in the dielectric constant. This added effect that goes beyond changing of the dielectric constant has been explained in terms of the preferential exclusion of alcohol from the vicinity of interacting DNA strands.⁶ These studies further demonstrated that because alcohol exclusion causes an additional osmotic pressure difference between the bulk solution and the concentrated DNA phase, DNA strands are pushed even closer together.

Two distinct features prevail when trying to model ions immersed in a binary solvent mixture within the standard Poisson–Boltzmann (PB) theory. First, the disparity between the solvent permeabilities leads to a *dielectrophoretic* force. The

* To whom correspondence should be addressed.
E-mail: andelman@post.tau.ac.il.

ensuing force acts on the solution, attracting the high permeability solvent (e.g., water) component toward the charged macromolecular surface and, at the same time, depleting the lower permeability one (e.g., alcohol). As a result, the solution becomes inhomogeneous and a permeability gradient is created in the vicinity of the charged interface, where the system favors the higher permeability component that can better screen the electrostatic field while excluding the low permeability solvent away from charged interfaces. The second important feature is the chemical (nonelectrostatic) preference of the ions for one of the two solvents. The dissolved ions effectively drag with them a solvation shell preferentially enriched in one of the solvents, thus repelling the second. When attracted to the oppositely charged surfaces, the dissolved ions thereby change the composition of the vicinal solvent. These two effects can enhance or compensate each other. In this work, we treat only the case where the two effects act synergistically to mutually enhance each other.

Previous theoretical works describing the effects of binary solvent mixtures dealt mainly with systems close to their critical point. Tsori and Leibler investigated the change in the phase transition temperature due to dielectric inhomogeneity and preferential solvation,¹³ while Onuki and Kitamura investigated corresponding surface tension and the ionic distribution near an interface.^{14–16} To contrast and compare, in the present work, we focus on binary solution systems in the single phase region and away from the coexistence region. Moreover, contrary to previous works, our main interest is the effect of the dielectrophoretic force and preferential solvation on the pressure (or forces) between two equally charged objects, such as a pair of charged DNA strands.

We model the system by delimiting ourselves to the simple planar geometry for two interacting macromolecular surfaces. Some experimental setups apply directly to this geometry and even for more complex setups, our model captures the essential physics of coupling between the binary solvents and mobile ions.

In what follows, we present a model where the ionic densities, the solvent relative composition, and the electrostatic potential are all continuous functions of the local position. We derive a set of coupled differential equations relating the various degrees of freedom at thermal equilibrium. Furthermore, we derive a general expression for the local pressure in the form of a modified contact theorem and provide proof that it is spatially homogeneous. This allows us to reduce the corresponding Poisson–Boltzmann equation to a first order differential equation that greatly simplifies the numerical problem.

Our numerical and analytical results focus on the solution mixtures where the low permeability solvent (alcohol) has a small concentration compared to the other solvent (water). First, we examine the influence of the various parameters on the composition profiles. We find that the deviation of the solvent composition profile from its average (bulk) value can lead to large deviations from the regular Poisson–Boltzmann theory predictions, especially regarding interactions between charged macromolecular surfaces. We investigate in detail the pressure dependence on the interplate separation and its sensitivity to controllable parameters, such as salt concentration and average solvent composition. Finally, we show a comparison between our pressure profiles and the relevant experiment on DNA.⁶

II. The Model

In the model considered here, ions are immersed in a binary mixture of two solvents confined between two planar charged

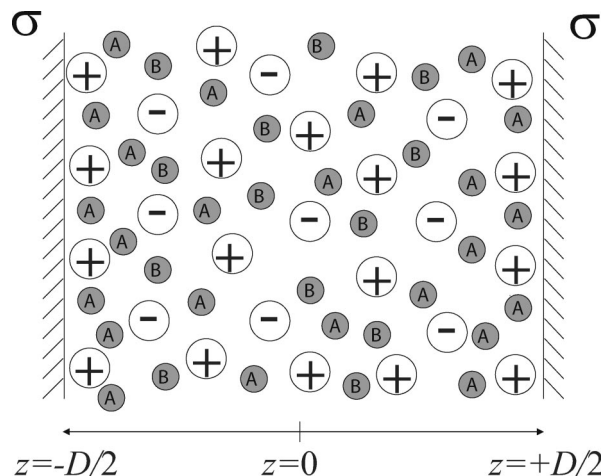


Figure 1. Schematic illustration of the model system. The two plates residing at $z = \pm D/2$ are charged with surface charge density $\sigma < 0$. The two solvents are represented by circles denoted A and B, with dielectric constants ϵ_A and $\epsilon_B < \epsilon_A$, respectively. The counterions and the high dielectric solvent (ϵ_A) are attracted to the plates.

interfaces. The two surfaces carry homogeneous surface charge densities, $\sigma < 0$ (see Figure 1). The model is formulated on a mean-field level but modifies the regular PB theory in two important aspects. First, the volume fractions of the two solvents, ϕ_A and $\phi_B = 1 - \phi_A$, are allowed to vary spatially. Consequently, the dielectric permeability of the binary mixture is also a function of the spatial coordinates. In the following, we assume that the local dielectric response $\epsilon(\mathbf{r})$ is a (linear) compositionally weighted average of the two permeabilities ϵ_A and ϵ_B :

$$\epsilon(\mathbf{r}) = \phi_A(\mathbf{r})\epsilon_A + \phi_B(\mathbf{r})\epsilon_B \quad (1)$$

or

$$\epsilon(\mathbf{r}) = \epsilon_0 - \phi(\mathbf{r})\epsilon_r \quad (2)$$

where we define $\phi \equiv \phi_B$, $\epsilon_0 \equiv \epsilon_A$, and $\epsilon_r \equiv \epsilon_A - \epsilon_B$. This linear interpolation assumption not only is commonly used but also is supported by experimental evidence.^{28,29} Note that the incompressibility condition satisfies $\phi_A + \phi_B = 1$, meaning that the ionic volume fractions are neglected.

Apart from long-range electrostatic interactions between dissolved ionic species, we also consider the case where short-range interactions make an important contribution to equilibrium properties. Consequently, pairwise short-range interactions between all constituents contribute additional terms to the total free energy and modify their equilibrium distributions, as will be elaborated below.

The equilibrium properties are derived within the mean-field framework. Thermodynamic equilibrium is obtained by minimizing the (grand canonical) thermodynamic potential, $G = \int d^3r g(\mathbf{r})$, leading to a generalized PB equation that also contains the contribution of short-range interactions. The force equilibrium leading to interactions between the confining surfaces is then obtained from the first integral of the PB equation and can be reduced to a surface-normal term of the generalized stress tensor evaluated at the bounding surfaces. The spatial profiles of the two solvents and ions, as well as the equilibrium forces, can be obtained from a variational principle of the thermodynamic potential.

A. Free Energy. We write the bulk free energy as a sum of four terms:

$$\int_V d^3r [f_e(\mathbf{r}) + f_i(\mathbf{r}) + f_m(\mathbf{r}) + f_s(\mathbf{r})] \quad (3)$$

where the free energy density $f = f_e + f_i + f_m + f_s$ and V is the total volume. The first term is due to electrostatic interactions between the ionic species mediated by the dielectric medium and characterized by the spatially inhomogeneous dielectric function $\varepsilon(\mathbf{r})$. For simplicity, the dissolved ions are assumed to result from a completely dissociated (1:1) monovalent salt. In this case, the electrostatic term, f_e , is given by

$$f_e = -\frac{\varepsilon(\mathbf{r})}{8\pi}(\nabla\psi)^2 + e(n_+ - n_-)\psi \quad (4)$$

where $\psi(\mathbf{r})$ is the electrostatic potential, e is the electron charge, and $n_{\pm}(\mathbf{r})$ is the number densities (per unit volume) of the monovalent co- and counterions. Note that the first term implicitly couples the electric field, $\mathbf{E} = -\nabla\psi$, with the solvent composition, $\phi(\mathbf{r})$, via the spatial dependence of the dielectric response, $\varepsilon(\mathbf{r})$, on local composition as was defined in eq 2. This is the dielectrophoretic term mentioned previously that favors a higher local dielectric constant (lower $\phi(\mathbf{r})$) and causes attraction of water to the charged surface. This is one of the two sources of the composition inhomogeneity in the model.

The entropy of ion mixing constitutes the second term, f_i , given by

$$f_i = k_B T [n_+(\log(n_+ a^3) - 1) + n_-(\log(n_- a^3) - 1)] \quad (5)$$

where k_B is the Boltzmann constant, T is the temperature, and a^3 is the molecular volume. The third term, f_m , accounts for the binary-mixture free energy given in our model by regular solution theory:

$$f_m = \frac{k_B T}{a^3} [\phi \log \phi + (1 - \phi) \log(1 - \phi) + \chi \phi(1 - \phi)] \quad (6)$$

The first two terms represent the solvent entropy of mixing, while the third represents the bilinear short-range interactions between the two solvents. The interaction parameter, χ , is dimensionless (rescaled by $k_B T$). Note that we took the same molecular volume a^3 for both A and B components. In general, this is not a serious deficiency and can be easily amended, if necessary.

The fourth term, f_s , in the free energy originates from the preferential interaction of the ions with one of the two solvents as described in the Introduction. We assume here that this preference can be described by a bilinear coupling between the two ion densities n_{\pm} and the relative solvent composition ϕ , which is the lowest order term that accounts for these interactions (higher order correlation terms can be added in a systematic way). The preferential solvation energy, f_s , is then given by

$$f_s = k_B T (\alpha_+ n_+ + \alpha_- n_-) \phi \quad (7)$$

where the dimensionless parameters α_{\pm} describe the solvation preference of the ions, defined as the difference between the

solute (free) energies dissolved in the A and B solvents. The free energy f_s corresponds closely to the Gibbs energy of transfer from one solvent to another, as is described in detail in refs 30 and 31. This bilinear coupling represents a second source of composition inhomogeneity. Namely, a density profile of the ions $n_{\pm}(\mathbf{r})$ (a diffusive layer near a charged object) forces a corresponding solvent profile, $\phi(\mathbf{r})$.

To all these bulk terms, one must add a surface term, describing the electrostatic interactions between charged solutes and confining charged interfaces. This surface term is given by

$$F_A = \oint_A d^2r e\sigma\psi_s \quad (8)$$

where ψ_s is the electrostatic potential evaluated at the bounding surfaces and depends on the surface charge density σ (charged groups per unit area) and surface area A . Note that the charged surface is described by a uniform charge density, σ . In a more refined model, nonelectrostatic interactions, such as preferential adsorption of the two solvents, and finite ion effects could be included as well.

The total free energy is then written as a sum of the bulk and surface terms

$$\int_V d^3r f(\psi, n_{\pm}, \phi) + \oint_A d^2r e\sigma\psi_s \quad (9)$$

In the grand-canonical ensemble, the corresponding thermodynamic potential is given by

$$g(\mathbf{r}) = f(\mathbf{r}) - k_B T \left[\mu_+ n_+(\mathbf{r}) + \mu_- n_-(\mathbf{r}) + \mu_{\phi} \frac{\phi(\mathbf{r})}{a^3} \right] \quad (10)$$

where μ_{\pm} and μ_{ϕ} are the dimensionless chemical potentials coupled to the ionic densities n_{\pm} and the relative solvent composition ϕ , respectively.

In thermodynamic equilibrium, the spatial profile of the various degrees of freedom characterizing the system is obtained by deriving the appropriate Euler–Lagrange (EL) equations via a variation principle of the thermodynamic potential, eq 10. The EL equations are then reduced to four coupled differential equations for the four degrees of freedom, $\psi(\mathbf{r})$, $n_{\pm}(\mathbf{r})$, and $\phi(\mathbf{r})$:

$$\nabla \cdot \left(\frac{\varepsilon}{4\pi} \nabla \psi \right) + e(n_+ - n_-) = 0 \quad (11)$$

$$\pm \frac{e\psi}{k_B T} + \log(n_{\pm} a^3) + \alpha_{\pm} \phi - \mu_{\pm} = 0 \quad (12)$$

$$\log\left(\frac{\phi}{1 - \phi}\right) + \frac{\varepsilon a^3}{8\pi k_B T} (\nabla\psi)^2 + \chi(1 - 2\phi) + a^3(\alpha_+ n_+ + \alpha_- n_-) - \mu_{\phi} = 0 \quad (13)$$

At the charged interfaces, an additional equation stems from the surface term of eq 9

$$\frac{\delta g}{\delta \psi_s} = 0 \Rightarrow \hat{\mathbf{n}} \cdot \nabla \psi \Big|_s = -\frac{4\pi e}{\varepsilon_s} \sigma \quad (14)$$

where \hat{n} is the unit vector normal to the bounding surfaces, $\varepsilon_s = \varepsilon_0 - \varepsilon_s \phi_s$ and ϕ_s are the surface values of ε and ϕ , respectively. The last equation, just as for standard PB theory, expresses the electroneutrality of the system, as can be shown by the integral form of Gauss law.

By solving the above set of equations, one can obtain the spatial profiles of the various degrees of freedom at thermodynamic equilibrium. For a general geometry, these equations can be solved only numerically.

B. Bulk Behavior. In the bulk, the system is homogeneous having a zero potential $\psi = 0$ and bulk values of $n_+ = n_- = n_b$ and $\phi = \phi_b$. The EL equations, eqs 11–13, reduce to

$$\begin{aligned} \log(n_b a^3) + \alpha_{\pm} \phi_b - \mu_{\pm} &= 0 \\ \log\left(\frac{\phi_b}{1 - \phi_b}\right) + \chi(1 - 2\phi_b) + a^3(\alpha_+ + \alpha_-)n_b - \mu_{\phi} &= 0 \end{aligned} \quad (15)$$

Eliminating the n_{\pm} fields, we remain with a single bulk equilibrium equation

$$\log\left(\frac{\phi_b}{1 - \phi_b}\right) + \chi(1 - 2\phi_b) + \Gamma e^{-1/2(\alpha_+ + \alpha_-)\phi_b} - \mu_{\phi} = 0 \quad (16)$$

where Γ is defined as

$$\Gamma = (\alpha_+ + \alpha_-) e^{1/2(\mu_+ + \mu_-)} \quad (17)$$

Depending on the values of μ_{ϕ} , μ_{\pm} , α_{\pm} , and χ , the solutions of the bulk equation correspond either to a single phase of density ϕ_b or to a coexistence between two phases with different densities. Hereafter, we restrict ourselves to the single-phase region of the phase diagram, where the chemical potentials μ_{\pm} and μ_{ϕ} follow directly from the form of the bulk free energy.

C. Planar Geometry. We exploit the symmetry of a planar system in order to derive analytically the pressure acting on the boundaries of the confined system. For a binary mixture confined to a slab delimited by two planar charged surfaces of infinite lateral extent (see Figure 1), the general treatment introduced above can be simplified, and the free energy can be cast into a one-dimensional integral over the normal \hat{z} direction. For this special case, we show next that the pressure is proportional to the first integral of the EL equations. Using this expression, we also derive a first-order differential equation for the electrostatic potential that will greatly simplify the problem.

1. Pressure in Planar Geometries. We start from a general form of the free energy F which depends on N one-dimensional fields $\{\psi_1(z), \dots, \psi_N(z)\}$ and their derivatives $\{\psi'_1(z), \dots, \psi'_N(z)\}$

$$F/A = \int dz f(\{\psi_i(z), \psi'_i(z)\}; z) \quad (18)$$

When f does not depend explicitly on the coordinate z , $\partial f/\partial z = 0$, we obtain the following relation (see Appendix A):

$$f - \sum_{i=1}^N \frac{\partial f}{\partial \psi_i} \psi'_i = \text{const} \quad (19)$$

In our problem, f can be written as a sum of electrostatic and nonelectrostatic contributions

$$f = -\frac{\varepsilon(\{n_i\})}{8\pi} \psi'^2 + \sum_{i=1}^N q_i n_i \psi + h(\{n_i\}) \quad (20)$$

where h is the grand potential of N different species with densities $\{n_1, \dots, n_N\}$ of a general form but without any electrostatic interactions. The charge of the i th species is denoted by q_i , and $\varepsilon(\{n_i\})$ is the dielectric response as a function of the densities $\{n_1, \dots, n_N\}$. Substituting eq 20 into eq 19, we obtain

$$-\frac{\varepsilon}{8\pi} \psi'^2 + \sum_{i=1}^N q_i n_i \psi + h + \frac{\varepsilon}{4\pi} \psi'^2 = \text{const} \quad (21)$$

Finally, using the equilibrium equations for the densities $\{n_1, \dots, n_N\}$

$$\frac{\partial f}{\partial n_i} = -\frac{1}{8\pi} \frac{\partial \varepsilon}{\partial n_i} \psi'^2 + q_i \psi + \frac{\partial h}{\partial n_i} = 0 \quad (22)$$

we end up with the following expression

$$\frac{1}{8\pi} \left[\varepsilon + \sum_i \frac{\partial \varepsilon}{\partial n_i} n_i \right] \psi'^2 + h - \sum_i n_i \frac{\partial h}{\partial n_i} = \text{const} \quad (23)$$

For the special case of noncharged liquid mixtures, f reduces to h , while it follows from general thermodynamic identities³² that the last two terms in eq 23 are equal to the negative of the local pressure

$$P = -h + \sum_i n_i \frac{\partial h}{\partial n_i} \quad (24)$$

However, even in a charged liquid mixture, the electrostatic potential vanishes away from the boundaries so that P is also the bulk value of the pressure in a charged system. Together with eq 21, it follows that the first integral can be cast into the form:

$$-P = \frac{1}{8\pi} \left[\varepsilon + \sum_i \frac{\partial \varepsilon}{\partial n_i} n_i \right] \psi'^2 + h - \sum_i n_i \frac{\partial h}{\partial n_i} \quad (25)$$

Namely, the integration constant of eq 23 is simply the negative of the pressure and is a constant throughout the system. We next consider separately the properties of the electrostatic and nonelectrostatic terms in eq 23.

The first term is nothing but the negative of the zz component of the Maxwell electrostatic stress tensor, appropriately generalized to the case where the dielectric permeability is density dependent.³³ The last two terms together, as already noticed, represent the local pressure of the system in the presence of charges. In the standard PB theory, these two terms are given by the van't Hoff form, while here they are given by an appropriate generalization, stemming from the free energy ansatz, eq 3. Combining all the terms in eq 23, we get the total zz component of the stress tensor, which in thermodynamic equilibrium has to be a constant and equal to $-P$, eq 25.

Note that the above proof is valid for any form of the free energy f (as h had an arbitrary form) and accounts for electrostatic as well as nonelectrostatic degrees of freedom in a completely general way. Applying this general result to our free energy, eqs 3–7, yields the following form of the total pressure:

$$P = -\frac{1}{8\pi}(\varepsilon_0 - 2\varepsilon_r\phi)\psi'^2 + k_B T \left(n_+ + n_- - \frac{\log(1 - \phi)}{a^3} \right) + k_B T \left(\alpha_+ n_+ \phi + \alpha_- n_- \phi - \frac{\chi\phi^2}{a^3} \right) \quad (26)$$

This pressure P should be compared with the pressure of the standard PB theory:

$$P_{\text{PB}} = -\frac{1}{8\pi}\varepsilon\psi'^2 + k_B T(n_+ + n_-) \quad (27)$$

and contains several additional terms. In fact, the difference between the two is twofold: first, a polarizability term of the form $\varepsilon_r\phi\psi'^2/4\pi$ is included in the pressure, since the dielectric constant is now spatially dependent. This term is equal to the product of the polarization $-\varepsilon_r\phi\psi'$ and the electric field $E = -\psi'$. Second, the short-range interactions also change the form of the pressure: the solvent interactions contribute the term $-\chi\phi^2/a^3$, and the ion–solvent interactions add the two terms, $\alpha_+n_+\phi$ and $\alpha_-n_-\phi$. This last addition changes the pressure significantly when considering two similarly charged surfaces. We will discuss this point at length below.

2. First Integral of the EL Equations in Planar Geometries.

We now use the form of the first integral of the EL equations (eq 26) to obtain an explicit first-order differential equation for the electric field. The EL equations for the ion densities, eq 12, give the following relations:

$$n_{\pm}(\psi, \phi) = n_b e^{\mp e\psi/k_B T - \alpha_{\pm}(\phi - \phi_b)} \quad (28)$$

From the first integral, we now deduce

$$\left(\frac{d\psi}{dz}\right)^2 = \frac{8\pi k_B T}{(\varepsilon_0 - 2\varepsilon_r\phi)} \left(n_+ + n_- - 2n_b + \alpha_+(n_+\phi - \phi_b n_b) + \alpha_-(n_-\phi - \phi_b n_b) + \frac{1}{a^3} \log \frac{1 - \phi_b}{1 - \phi} - \frac{1}{a^3} \chi(\phi^2 - \phi_b^2) - n_b \Pi \right) \quad (29)$$

The difference between the pressure P at finite separation and its bulk value P_b (infinite separation) is given by the rescaled osmotic pressure $\Pi = (P - P_b)/k_B T n_b$ and

$$\frac{P_b}{k_B T n_b} = 2 + (\alpha_+ + \alpha_-)\phi_b - \frac{1}{a^3 n_b} \log(1 - \phi_b) - \frac{1}{a^3 n_b} \chi\phi_b^2 \quad (30)$$

For a single plate (or, equivalently in the limit of two plates at infinite separation), Π vanishes. Note that n_{\pm} in eq 29 are functions of ϕ and ψ , and ϕ is by itself a function of ψ and ψ' ,

given by eq 13 that is a transcendental algebraic equation for ϕ :

$$\frac{\varepsilon_r}{8\pi k_B T} \left(\frac{d\psi}{dz}\right)^2 + \alpha_+(n_+ - n_b) + \alpha_-(n_- - n_b) + \frac{1}{a^3} \left(\log \frac{\phi}{1 - \phi} - \log \frac{\phi_b}{1 - \phi_b} - 2\chi(\phi - \phi_b) \right) = 0 \quad (31)$$

The boundary conditions for each plate/boundary are given by three coupled algebraic equations for ϕ_s , ψ_s , and ψ'_s . The first two equations are eqs 29 and 31. The third equation is given by the electroneutrality condition, eq 14, that can be simply rewritten in the form

$$\varepsilon_s \psi'_s + 4\pi e\sigma = 0 \quad (32)$$

and ε_s was defined after eq 14.

III. Results and Discussion

The equilibrium equations eqs 29, 31, and 32 derived above have no closed analytical solution. Hence, we solve them numerically to obtain spatial profiles for ϕ and n_{\pm} . In addition, by considering the new terms as small perturbations (compared to the regular PB theory), we show that an approximate analytical solution can be derived for the single plate case in the absence of salt. We then show numerical results for the pressure as a function of separation and for the pressure dependence on the experimentally controlled parameters α_+ , ϕ_b , and n_b . Lastly, we compare our results to one available set of experiments on DNA in a binary solvent mixture.

A. Density and Permeability Profiles. We investigate the limit of small concentrations of the low dielectric component with no preferential solvation interactions ($\alpha_{\pm} = 0$) and for two values of the χ parameter. In Figure 2, we compare these numerical solutions for a single surface (for which the osmotic pressure vanishes, $\Pi = 0$, similar to infinite interplate separation) to the ones of the regular PB equation with a homogeneous (average) dielectric constant, $\varepsilon_{\text{av}} \equiv \varepsilon_A - \phi_b(\varepsilon_A - \varepsilon_B)$.

When all additional interactions are omitted ($\alpha_{\pm} = 0$ and $\chi = 0$), the difference between the two models is negligible. While the deviation in ϕ right at the surface reaches 10% of its bulk value ϕ_b , it leads to only a 0.5% deviation for the dielectric constant ε at the surface. The dependence of the other fields ψ and n_{\pm} on ϕ is only due to changes in the dielectric constant. Therefore, in the limit of no short-range interactions, these fields hardly differ from the results of the regular PB model with homogeneous dielectric constant ε_{av} . The correction due to addition of solvent short-range interactions is also found to be small, even for larger solvent–solvent interaction, $\chi = 1.5$. This χ value still describes a single bulk phase, as it is smaller than the critical value $\chi_c = 2$. We conclude that, in the absence of preferential solvation, $\alpha_{\pm} = 0$, the modified PB model has only a small added effect on the permeability, as can be seen in Figure 2.

In Figure 3, we examine numerically the effect of preferential solvation on the solvent profile in the low concentration limit ($\phi_b = 0.09$). Simply stated, when the ions prefer to be in the vicinity of the high permeability solvent molecules, we expect an increase in the exclusion of the low permeability solvent near the wall. Indeed, as can be seen in Figure 3, the exclusion of the low permeability solvent increases with α_+ . We also find

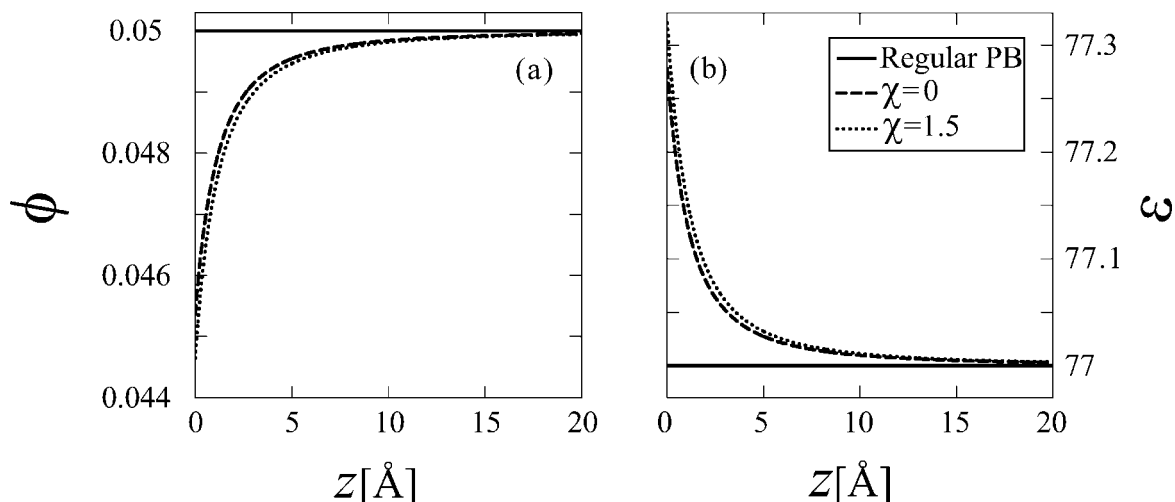


Figure 2. Spatial profiles of (a) the solvent relative composition ϕ and (b) the permeability ε . The regular PB with homogeneous dielectric constant $\varepsilon = 77$ (solid line) is compared with our modified PB for binary mixture with and without short-range interactions, $\chi = 0$ (dashed line) and $\chi = 1.5$ (dotted line), respectively. Other parameters are $\sigma = -1/100 \text{ \AA}^{-2}$, $n_b = 10^{-4} \text{ M}$, $\varepsilon_A = 80$, $\varepsilon_B = 20$, and $\phi_b = 0.05$. In all the cases, no preferential solvation is considered, $\alpha_{\pm} = 0$.

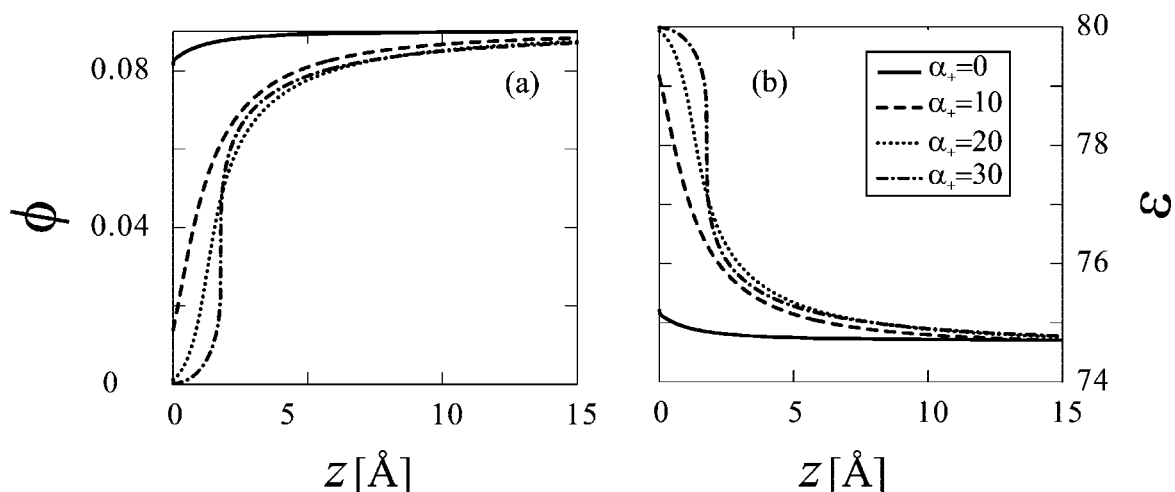


Figure 3. Spatial profiles of (a) the solvent composition ϕ and (b) the dielectric constant ε for various values of α_+ as shown in the legend. The co-ion parameter is $\alpha_- = 0$, the surface charge density is $\sigma = -1/100 \text{ \AA}^{-2}$, and the salt concentration is $n_b = 10^{-4} \text{ M}$. The solvent dielectric constants are $\varepsilon_A = 80$ and $\varepsilon_B = 20$. The bulk value of ϕ is $\phi_b = 0.09$.

that the value of the co-ion–solvent short-range interaction parameter α_- does not significantly affect the form of the permeability profile and is set hereafter to zero.

Moreover, when increasing α_+ even further ($\alpha_+ = 30$ in Figure 3), $\phi(z)$ and $\varepsilon(z)$ have a sharp change at about $z = 2 \text{ \AA}$. Namely, a layer rich in A species is formed near the wall with a thickness of a few angstroms, and at a certain distance from the wall ϕ decreases abruptly to a value close to the bulk value ϕ_b . This phenomenon is clearly a consequence of the $n_+\phi$ coupling and is in itself not an electrostatic effect. A gradient squared term $(\nabla\phi)^2$ in the free energy would have smoothed out this behavior and will be considered elsewhere. The steep variation observed for the nonhomogeneous mixture could be due to the fact that the boundary condition demands a ϕ value that is much different from the one that follows from the bulk equation (eq 16), so that the system tends to exhibit bulklike behavior as soon as possible. A detailed analysis of this phenomena will be presented in a separate study.

B. Some Analytic Results. The model described above can be solved analytically by making some simplifying assumptions,

and considering certain limiting behaviors. We assume that there are no solvent short-range interactions ($\chi = 0$) and that the preferential solvation interaction is weak compared to $k_B T$ ($\alpha_+ \ll 1$). We also assume that the contribution due to the permeability inhomogeneities is negligible, and take ε throughout the system to be the weighted average of the two bulk relative compositions, ε_{av} . Moreover, we take the limit of zero salt, as if only counterions are present to keep the system neutral. Lastly, we assume that one of the solvent concentrations is much smaller than the other.

With these assumptions, we can practically isolate the effect of preferential solvation and obtain analytical profiles. The PB equation in this limit assumes the form

$$\frac{d^2\psi}{dz^2} = -\frac{4\pi en(z)}{\varepsilon_{av}} \quad (33)$$

where the ion density $n(z)$ is a function of both the potential ψ and the solvent relative composition ϕ

$$n(z) = n_b e^{-e\psi/k_B T - \alpha(\phi - \phi_b)} \quad (34)$$

The prefactor n_b is determined by satisfying the electroneutrality condition, and the subscript \pm in n_{\pm} is omitted in this counterion only case.

The composition ϕ as a function of n is

$$\phi = \phi_b e^{-\alpha a^3 n} \approx \phi_b (1 - \alpha^3 a^3 n) \quad (35)$$

Here, we made use of the assumption that the preferential solvation interaction is small, $\alpha(a^3 n) \ll 1$. Substituting it back into eq 34, we obtain for the further limit, $\alpha\phi \ll 1$,

$$n = \frac{n_b e^{-e\psi/k_B T}}{1 - \alpha^2 a^3 \phi_b n_b e^{-e\psi/k_B T}} \quad (36)$$

For finite values of $e\psi/k_B T$ and in the limit of $\alpha^2 \phi_b a^3 n_b \ll 1$, we obtain to lowest order

$$n \approx n_b e^{-e\psi/k_B T} (1 + \alpha^2 \phi_b a^3 n_b e^{-e\psi/k_B T}) \quad (38)$$

Using this equation in the PB equation, we get a second order differential equation for ψ :

$$\frac{d^2 \psi}{dz^2} = -\frac{4\pi e n_b}{\epsilon} (e^{-e\psi/k_B T} + \alpha^2 \phi_b a^3 n_b e^{-2e\psi/k_B T}) \quad (39)$$

For a single plate, the boundary condition to the equation above is given by

$$\left. \frac{e}{k_B T} \frac{d\psi}{dz} \right|_{z=0} = 4\pi l_B |\sigma| \equiv \frac{2}{\lambda_{GC}} \quad (40)$$

where $l_B = e^2/\epsilon_a k_B T$ and λ_{GC} is the well-known Gouy–Chapman (GC) length.¹⁰

Solving the equation above, we obtain the following results:

$$\psi(z) = \frac{k_B T}{e} \log[(z + \lambda_{GC}^m)^2 - \lambda_s^2] + \psi_0 \quad (41)$$

$$n(z) = \frac{(z + \lambda_{GC}^m)^2 + \lambda_s^2}{2\pi l_B [(z + \lambda_{GC}^m)^2 - \lambda_s^2]^2} \quad (42)$$

where $\lambda_s^2 = \alpha^2 a^3 \phi_b / 4\pi l_B$ is a typical length associated with the α parameter. The second length scale is the modified Gouy–Chapman (GC) length λ_{GC}^m obtained by satisfying the boundary condition:

$$\lambda_{GC}^m = \frac{\lambda_{GC}}{2} (1 + \sqrt{1 + 4(\lambda_s/\lambda_{GC})^2}) \quad (43)$$

For $\lambda_s \ll \lambda_{GC}$, one obtains $\lambda_{GC}^m \approx \lambda_{GC} [1 + (\lambda_s/\lambda_{GC})^2]$. Thus, the effect of preferential solvation enhances the ion density in the proximity of the surface, and results in a faster decay of the density profile.

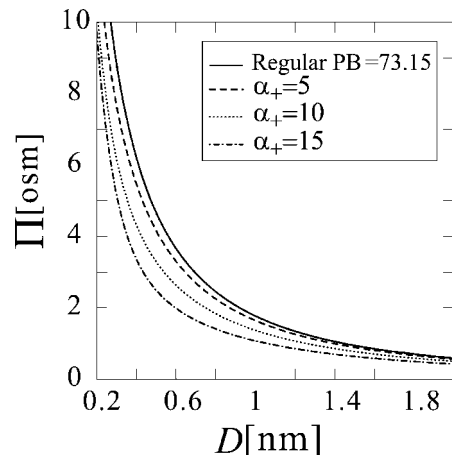


Figure 4. Dependence of pressure on separation D for various ion–solvent interaction strengths α_+ as shown in the legend. Other parameters are $\sigma = -1/100 \text{ \AA}^{-2}$, $n_b = 10^{-4} \text{ M}$, $\epsilon_A = 80$, $\epsilon_B = 4$, and $\phi_b = 0.09$.

C. Pressure versus Separation Curves. Due to symmetry, the pressure between two identically charged plates is most conveniently calculated at the midplane. When considering the change in pressure due to the permeability inhomogeneity, one can separate the direct and indirect corrections. The direct one is due to the change of midplane composition $\phi(z)$, while the indirect one is related to changes of the midplane ion density. In the absence of preferential solvation ($\alpha_{\pm} = 0$), ϕ at the midplane depends only on the local value of the electrostatic field (see eq 31 with $\alpha_{\pm} = 0$). However, in a symmetric two-plate system, the electrostatic field vanishes at the midplane and ϕ there equals to its bulk value, ultimately contributing no correction to the pressure. Moreover, since $\epsilon(z)$ turns out to be nearly homogeneous (see Figure 2), the indirect correction is minute as well. Thus, in the absence of preferential solvation the combined effect of a binary mixture is negligible.

When adding the preferential solvation term characterized by the parameter α_{\pm} (the term coupling between n_{\pm} and ϕ), ϕ becomes dependent on the nonzero midplane potential. As a consequence, the midplane ϕ value differs from ϕ_b and results in two direct corrections to the pressure. The first comes from the osmotic pressure of the solvent ($\sim k_B T (\phi - \phi_b) / a^3$), while the second originates from the ϕn_{\pm} coupling term. Thus, even if the indirect contribution to the profiles is negligible, the direct correction alone can substantially change the pressure.

The effect of preferential solvation on the pressure between two identically charged surfaces is now examined for various values of the α_+ parameter. As the coupling term in eq 26 contributes directly to the pressure, the effect of changing α_+ is rather pronounced in the pressure versus separation curves (see Figure 4). The figure clearly shows that the pressure decreases when α_+ increases. Yet, because the effect is short ranged, the major differences are observed at small separations ($D < 2 \text{ nm}$). From the analysis of the profiles with respect to the interaction strength (Figure 4), we conclude that the change in pressure is substantial only up to distances of a few nanometers. This means that for large separations the midplane values of the fields ψ , n , and ϕ within our model will be similar to the regular PB theory predictions. However, for small separations of the order of 1–2 nm, both the profiles and the pressure are affected by the preferential solvation.

D. The Effect of the Solution Parameters on the Pressure. We proceed by examining the influence of the parameters α_+ , ϕ_b , and n_b on the pressure. The α_+ parameter can be modified

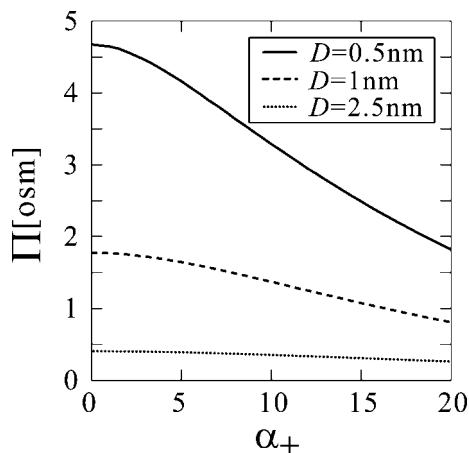


Figure 5. Pressure as a function of α_+ for various interplate separations: $D = 0.5, 1,$ and 2.5 nm. Other parameters are $\sigma = -1/100 \text{ \AA}^{-2}$, $n_b = 10^{-5} \text{ M}$, $\epsilon_A = 80$, $\epsilon_B = 4$, and $\phi_b = 0.09$.

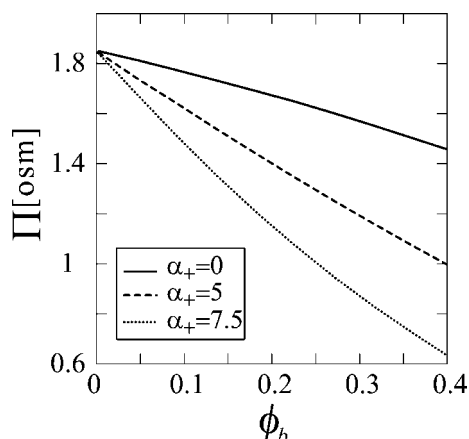


Figure 6. Pressure versus bulk solvent composition ϕ_b for various ion-solvent interaction strength, α_+ . Other parameters are $\sigma = -1/100 \text{ \AA}^{-2}$, $n_b = 10^{-5} \text{ M}$, $\epsilon_A = 80$, and $\epsilon_B = 4$. The separation is fixed at $D = 1$ nm.

experimentally by using different solvents, while ϕ_b and n_b can be easily controlled in the experiment by changing composition.

In Figure 5, we present the dependence of the pressure $\Pi(\alpha_+; D)$ on the interaction strength α_+ for a fixed separation. As expected, for small values of α_+ (< 2), the pressure depends only weakly on the interaction strength, whereas for larger values the pressure falls with α_+ . This implies that there is a value of α_+ where its direct contribution to the pressure becomes larger than all other contributions (electrostatic and entropic). Moreover, the slope of $\Pi(\alpha_+; D)$ depends on the separation, as can be clearly seen by comparing the $D = 0.5$ nm and $D = 1$ nm results. For smaller separations ($D = 0.5$ nm), the preferential solvation effect is stronger in accordance with the results shown in the previous sections (Figures 2–4), where the effect has a range of a few nanometers. For $D = 2.5$ nm, the pressure changes very slowly with α_+ and the preferential solvation is small even for large α_+ ($15 < \alpha_+ < 20$).

Next, we investigate how increasing ϕ_b changes the pressure. In Figure 6, we plot the pressure versus ϕ_b for a fixed separation $D = 1$ nm for three values of the interaction strength α_+ . Increasing the low permeability solvent concentration decreases the pressure through decrease of the permeability and by increasing the preferential solvation. The results in Figure 6 suggest that even for $\alpha_+ = 0$ (no preferential solvation) the pressure decreases with ϕ_b , implying that the dielectrophoretic mechanism contributes a nearly linear dependence on ϵ_r . When

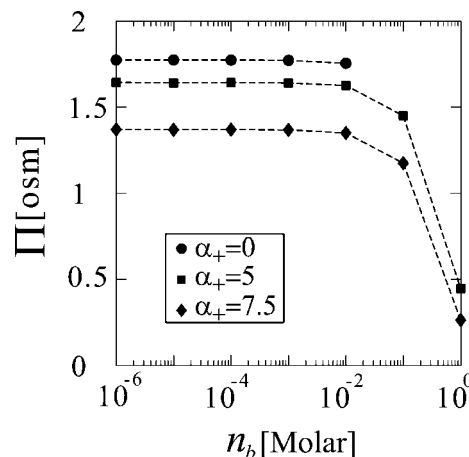


Figure 7. Pressure versus bulk salt concentration n_b for various ion-solvent interaction strength, α_{\pm} . Other parameters are $\sigma = -1/100 \text{ \AA}^{-2}$, $\epsilon_A = 80$, $\epsilon_B = 4$, and $\phi_b = 0.09$. The separation is fixed at $D = 1$ nm. Lines are guides for the eye.

increasing α_+ , the $\Pi(\phi_b)$ slope is steeper due to higher bulk pressure of the low permeability solvent, contributing directly to the pressure through the preferential solvation term (eq 26).

Since there is a linear ϕ_b term in the pressure ($\sim -k_B T \phi_b / a^3$), one can deduce from the results above that the main contribution to the pressure comes simply from a higher reference concentration ϕ_b that reduces the pressure. Namely, for small separations, the solvent ϕ and the ion n_{\pm} at the midplane have only a weak dependence on ϕ_b , similar to regular PB theory where the pressure has no dependence on the bulk salt density n_b at small separations.¹⁰

Finally, we investigate the influence of the salt concentration on the pressure at fixed separation ($D = 1$ nm). The results are presented in Figure 7, where we plot the pressure versus the salt concentration for fixed separation and for different values of the interaction strength α_+ . For low concentration ($n_b < 10^{-2} \text{ M}$), the pressure has no dependence on n_b . It is known from the regular PB theory¹⁰ that, at small separations, when the Debye length is much larger than the separation ($\lambda_D \gg D$), the pressure only weakly depends on the salt concentration. In this sense, the modified PB theory presented here is similar to the regular PB theory. The effect of preferential solvation is just a constant addition to the pressure, which keeps the same dependence of the pressure on the salt concentration. When going to larger concentrations, where the Debye length becomes comparable to or smaller than the separation, the pressure decays exponentially as can be expected also from standard PB theory.

E. Comparison of Model with Experiment. So far, we have shown that we are able to account for some of the forces that lead to cosolvent preferential exclusion from charged interacting macromolecular surfaces. In particular, our model accounts not only for locally varying dielectric profiles that follow the solvent mixture composition (through the variables ϵ_A and ϵ_B), but also for preferential ion solvation (through the variables α_{\pm}), that in turn depends on local solvent composition as well. Using these two sets of parameters, it is possible to propose a physical mechanism for solute (or solvent) exclusion from interacting surfaces. The different dielectric constants of the two solvent components cause depletion of one of the components from the charged surface. This variation in solvent composition can in turn affect the concentration of ions between the two interacting surfaces. The combined effect can lower the disjoining pressure between equally charged surfaces by varying local solution concentrations.

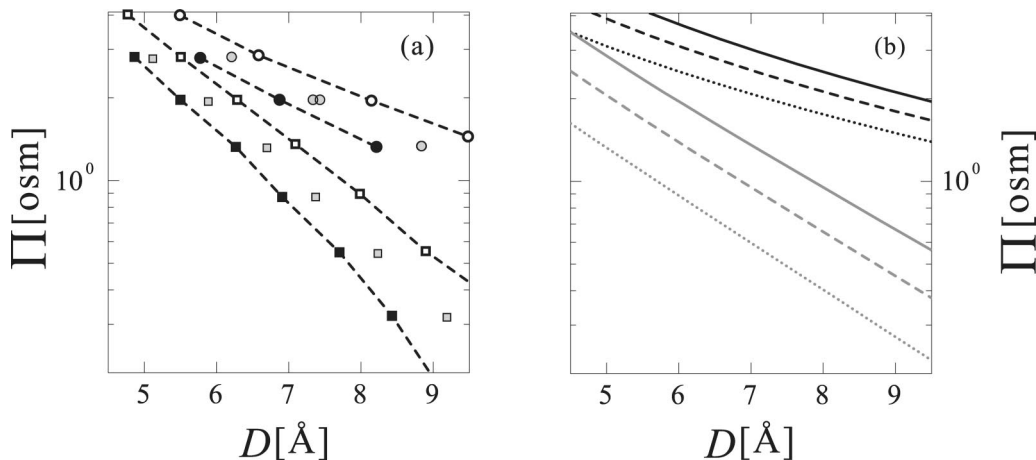


Figure 8. Pressure Π as a function of the separation D . (a) Experimental data. Circles (squares) represent the 0.02 M (1.2M) added NaBr salt results adopted from ref 6. Empty circles and squares represent the experiment with no MPD. Gray circles and squares represent the experiment with 0.5 M MPD. Black circles and squares represent the experiment with 1 M MPD. The dashed lines are guides to the eye. (b) Numerically calculated lines from the model with parameters taken to match the experiment. Ion–solvent interaction strength is the same for all lines $\alpha_+ = 5$, and it was treated as a fitting parameter. The surface charge is taken as $\sigma = -1/100 \text{ \AA}^{-2}$ to fit the DNA values. The dielectric constants are $\epsilon_A = 80$ (water) and $\epsilon_B = 25$ (MPD). Black lines are for $n_b = 0.02 \text{ M}$, and gray lines are for $n_b = 1.2 \text{ M}$. Solid, dashed, and dotted lines stand for $\phi_b = 0.0018$, $\phi_b = 0.126$, and $\phi_b = 0.252$, respectively.

While it is hard to unambiguously prove the origins of the molecular interactions that lead to the different solvation properties of ions and cosolvent in the vicinity of complex macromolecules, we show that by varying the model parameters we can account for the observed trends in the experimental studies of Rau and Stanely.⁶ In these experiments, osmotic pressure is applied to a condensed phase of DNA strands in aqueous solution by adding a neutral polymer, poly(ethylene glycol) (PEG) that is completely excluded from the DNA phase. The DNA–DNA spacings in solution, D , are measured using small-angle X-ray scattering. In addition, salt and different alcohols are added at different concentrations. Figure 8a shows the experimentally derived $\Pi(D)$ (equation of state) for DNA solutions containing either 0.02 or 1.2 M NaBr salts, as they appear in ref 6. Solutions to which 2-methyl-2,4-pentanediol (MPD) alcohol was added at concentrations of 0.5 or 1 M are compared with solution with no MPD. As the figure shows, for both salt concentrations, the added salt lowers the DNA–DNA spacing for a particular applied osmotic pressure. However, the figure also clearly shows that the reduction in Π is more significant at the higher salt concentration. This would imply that salts (or more generally electrostatic forces) are involved in determining the effect of MPD on Π , suggesting an important role reserved for the dielectric properties that can be linked to the distribution of ions and cosolvent partitioning in between the DNA strands.

Even though our model considers interactions between flat surfaces, rather than the cylindrical ones expected for DNA strands, we show that it is possible to get similar trends to those found in experiment using the two sets of the ϵ and α parameters. Figure 8b shows our results for two charged plates with charge density similar to that of DNA ($\sigma = -1/100 \text{ \AA}^{-2}$) and dielectric constants of $\epsilon_A = 80$ (representing water) and $\epsilon_B = 25$ (close to the value of pure MPD). In our model, we use only the relative volume fraction ϕ_b of the two species, water and MPD, without accounting for their different molar weight (water molar weight is 18 and that of MPD is 118). In the experiment,⁶ the two MPD solutions have concentrations of 0.5 and 1.0 M corresponding, respectively, to $\phi_b = 0.055$ and 0.11. These values are in good agreement with the values chosen in our model (Figure 8b) to give a good fit to the experimental

data: $\phi_b = 0.126$ and 0.252. Note that the value $\phi_b = 0.0018$ is chosen for convenience to fit the zero MPD concentration case. The value of α_+ could, in principle, be evaluated from the solvation free energy of NaBr salts in binary water–MPD solutions of different contents. Because such data is lacking, we treat α_+ as a fitting parameter and use $\alpha_+ = 5$ (in units of $k_B T$), allowing us to fit closely the experimental data. We note that this α_+ value is close to the experimental transfer free energy of sodium from water to ethanol $\sim 5k_B T$ as was quoted in ref 31. The value of α_- for bromide, which was taken in our work as zero, seems to be generally lower than that of α_+ but is less clearly resolved.³⁰

We find that for this set of parameters the numerical calculation *grasso modo* follows the experimental trends: the spacing between curves grows with equal additions of alcohol to the solution, but for the higher salt concentration the change in Π is larger. These results underscore two important general conclusions. First, it would be impossible to explain the difference in the $\Pi(D)$ behavior for high salt versus low salt without discussing ions and the role of the dielectric medium. Our model introduces these species in a self-consistent manner through the PB-like theory. Second, the comparison demonstrates the important role reserved for the preferential ion-solvation interactions in the different components of the binary solution. Specifically, it would be impossible to explain the shifts in distances at a given applied osmotic stress without invoking a nonzero α_+ , that in turn shifts the exclusion of ions due to changes in solution composition in the DNA phase.

IV. Conclusions

The model presented in this work is a modification of the regular PB theory and accounts for the effects of a dielectric medium composed of two solvents. There are two important features that modify the standard PB theory. Due to different dielectric constants of the two solvents, the permeability is no longer homogeneous. This effect is accounted for by coupling the electrostatic field to the solvent local composition. The second modification is the addition of a preferential solvation term which enables the ions to drag a favorable solvent and locally deplete the other. This is modeled by a coupling term

between the ion density and the solvent local composition. Similar models can be used for a number of problems such as the properties of interfaces,^{15,16} the critical behavior of binary mixture in the presence of ions,^{13,14} and the forces between more elaborated charged macromolecules, which is the main focus of this work.

For two identically charged planes, we find that, in the absence of preferential solvation, the density profiles and the pressure undergo only small modifications. This is demonstrated numerically and supported by an argument that relies on the symmetry of the two-plate system. However, by adding the preferential solvation term, we are able to observe a considerable correction to the pressure at small separations. The coupling between ion density and solvent local composition appreciably changes the midplane concentration values, and as a consequence the pressure is reduced. We also investigated the dependence of the pressure on experimentally controlled parameters such as salt concentration, bulk solvent composition, and preferential solvation strength. The pressure depends on the preferential solvation but changes substantially only at small separations (1–2 nm). The threshold of preferential solvation energy which is required to change the pressure significantly is on the order of a few $k_B T$. It is found that the pressure depends nearly linearly on the bulk relative composition, implying that the density profiles at small separations have no dependence on ϕ_b . Finally, the effect of added salt to the solution seems to change the pressure in the same manner as for regular PB theory.

We also used our model to put fourth an explanation for the experimentally measured pressures in a condensed phase of DNA. The comparison shows that the experimental trend is borne out by our model results. This suggests that the main mechanism causing the depletion of one solvent away from the charged macromolecule is very plausibly the preferential solvation of the ions. Thus, beyond simple electrostatic screening, salt ions may play an additional and important role in the behavior of charged macromolecules immersed in solution.

Further applications and refinements of the model could be considered. For example, the model can be used to analyze the effect of strong preferential solvation on the critical behavior. As shown in Figure 3, the solvent relative composition profile becomes discontinuous at strong preferential solvation. We believe that this can be explained in the framework of a Ginzburg–Landau theory that would account for the phase transition. Moreover, in addition to the simple planar geometry treated here, other geometries such as a cylindrical one can obtain a more direct quantitative comparison with DNA experiments. Finally, the limit of ionic dilute solutions can be generalized to the concentrated limit, including the full entropy of mixing, as was considered in ref 34.

Acknowledgment. We thank Ariel Abrashkin, Adrian Parsegian and Yoav Tsori for numerous discussions. We are indebted to Don Rau and Brian Todd for helpful discussions and for sharing experimental data with us. D.A. acknowledges support from the Israel Science Foundation (ISF) under Grant No. 231/08 and the U.S.–Israel Binational Foundation (BSF) under Grant No. 2006/055. R.P. and D.H. would like to acknowledge the support from the Israeli and Slovenian Ministries of Science through a joint Slovenian–Israeli research grant. The Fritz Haber research center is supported by the Minerva foundation, Munich, Germany. This study was in part supported by the Intramural Research Program of the NIH,

Eunice Kennedy Shriver National Institute of Child Health and Human Development.

Appendix A: Derivation of Pressure in One-Dimensional System

In the following we present the derivation of eq. 19. We start from a free energy F , eq 18 which depends on N coupled one-dimensional fields $\{\psi_1(z), \dots, \psi_N(z)\}$ and their derivatives $\{\psi'_1(z), \dots, \psi'_N(z)\}$:

$$F/A = \int f(\{\psi_i(z), \psi'_i(z)\}; z) dz \quad (\text{A1})$$

where $i = 1, \dots, N$. There are N EL equations

$$\frac{\delta F}{\delta \psi_i} = 0 \Rightarrow \frac{\partial f}{\partial \psi_i} - \frac{d}{dz} \frac{\partial f}{\partial \psi'_i} = 0 \quad (\text{A2})$$

The total derivative of $f(z)$ is

$$\frac{df}{dz} = \sum_i \left(\frac{\partial f}{\partial \psi_i} \psi'_i + \frac{\partial f}{\partial \psi'_i} \psi''_i \right) + \frac{\partial f}{\partial z} \quad (\text{A3})$$

Moreover, we can write

$$\frac{\partial f}{\partial \psi'_i} \psi''_i = \frac{d}{dz} \left(\frac{\partial f}{\partial \psi'_i} \psi'_i \right) - \frac{d}{dz} \left(\frac{\partial f}{\partial \psi'_i} \right) \psi'_i \quad (\text{A4})$$

Substituting this back into eq A3 and using the EL equations we find

$$\frac{df}{dz} = \sum_i \left[\frac{d}{dz} \left(\frac{\partial f}{\partial \psi'_i} \psi'_i \right) \right] + \frac{\partial f}{\partial z} \quad (\text{A5})$$

When $f(z)$ does not depend explicitly on the coordinate z , $\partial f / \partial z = 0$, the last term vanishes and we end up with a first order differential relation:

$$f - \sum_i \left(\frac{\partial f}{\partial \psi'_i} \psi'_i \right) = \text{const.} \quad (\text{A6})$$

References and Notes

- (1) Israelachvili, J. N.; McGuigan, P. M. *Science* **1988**, *241*, 795.
- (2) Rand, R. P.; Parsegian, V. A. *Biochim. Biophys. Acta, Biomembr.* **1989**, *988*, 351.
- (3) Ducker, W. A.; Senden, T. J.; Pashley, R. M. *Langmuir* **1992**, *8*, 1831.
- (4) Parsegian, V. A.; Rand, R. P.; Rau, D. C. *Proc. Natl. Acad. Sci. U.S.A.* **2000**, *97*, 3987.
- (5) Hultgren, A.; Rau, D. C. *Biochemistry* **2004**, *43*, 8272.
- (6) Stanely, R.; Rau, D. C. *Bipophys. J.* **2006**, *91*, 912.
- (7) Chik, J.; Mizrahi, S.; Chi, S.; Parsegian, V. A.; Rau, D. C. *J. Phys. Chem. B* **2005**, *109*, 9111.
- (8) Bonnet-Gonnet, C.; Leikin, S.; Chi, S.; Rau, D. C.; Parsegian, V. A. *J. Phys. Chem. B* **2001**, *105*, 1877.
- (9) Israelachvili, J. N. *Intermolecular and Surface forces*, 2nd ed.; Academic: London, 1992. Evans, D. F.; Wennerström, H. *The Colloidal Domain*; VCH: New York, 1994.
- (10) Andelman, D. In *Handbook of Physics of Biological Systems*; Lipowsky, R., Sackman, E., Eds.; Elsevier Science: Amsterdam, 1995; Vol. I, Chap. 12. Andelman, D. In *Soft condensed matter physics in molecular and cell biology*; Poon, W., Andelman, D., Eds.; Taylor & Francis: New York, 2006; pp 97–122.

- (11) Henderson, D. *Fundamentals of Inhomogeneous Fluids*; Dekker: New York, 1992.
- (12) Netz, R. R.; Andelman, D. *Phys. Rep.* **2003**, *380*, 1.
- (13) Tsori, Y.; Leibler, L. *Proc. Natl. Acad. Sci. U.S.A.* **2007**, *104*, 7348.
- (14) Onuki, A.; Kitamura, H. *J. Chem. Phys.* **2004**, *121*, 3143.
- (15) Onuki, A. *Phys. Rev. E* **2006**, *73*, 021506.
- (16) Onuki, A. *J. Chem. Phys.* **2008**, *128*, 224704. Abrashkin, A.; Andelman, D.; Orland, H. *Phys. Rev. Lett.* **2007**, *99*, 077801.
- (17) Rubinstein, M.; Colby R. *Polymer Physics*; Oxford University: Oxford, U.K., 2003.
- (18) Squires, T. M.; Quake, S. R. *Rev. Mod. Phys.* **2005**, *77*, 977.
- (19) Gravesen, P.; Branebjerg, J.; Jensen, O. S. *J. Micromech. Microeng.* **1993**, *3*, 168.
- (20) Whiteside, G. M. *Nature* **2006**, *442*, 368.
- (21) Psaltis, D.; Quake, S. R.; Yang, C. *Nature* **2006**, *442*, 381.
- (22) Timasheff, S. N. *Annu. Rev. Biophys. Biomol. Struct.* **1993**, *22*, 67.
- (23) Davis-Searles, P. R.; Saunders, A. J.; Erie, D. A.; Winzor, D. J.; Pielak, G. J. *Annu. Rev. Biophys. Biomol. Struct.* **2001**, *30*, 271.
- (24) Record, M. T.; Zhang, W., Jr.; Anderson, C. F. *Adv. Protein Chem.* **1998**, *51*, 281.
- (25) Bolen, D. W.; Baskakov, I. V. *J. Mol. Biol.* **2001**, *310*, 955.
- (26) Harries, D.; Rösgen, J. *Methods Cell Biol.* **2008**, *84*, 679.
- (27) Baigl, D.; Yoshikawa, K. *Biophys. J.* **2005**, *88*, 3486.
- (28) Arakawa, T.; Timasheff, S. N. *Methods Enzymol.* **1985**, *114*, 49.
- (29) McPherson, A. *Methods Enzymol.* **1985**, *114*, 120.
- (30) Marcus, Y. *Chem. Rev.* **2007**, *107*, 3880.
- (31) Kalidas, C.; Hefter, G.; Marcus, Y. *Chem. Rev.* **2000**, *100*, 819.
- (32) Rowlinson, J. S.; Widom, B. *Molecular Theory of Capillarity*; Oxford University: Oxford, 1989.
- (33) Landau, L. D.; Lifshitz, E. M. *Electrodynamics of Continuous Media*; Pergamon Press: Oxford, 1975.
- (34) Borukhov, I.; Andelman, D.; Orland, H. *Phys. Rev. Lett.* **1997**, *79*, 435. Borukhov, I.; Andelman, D.; Orland, H. *Electrochim. Acta* **2000**, *46*, 221.

JP9003533